Title
Effect of the Mitral Valve's Anterior Leaflet on Axisymmetry of Transmitral Vortex Ring

Journal
Annals of Biomedical Engineering, 43(10)

ISSN
0145-3068

Authors
Falahatpisheh, Ahmad
Pahlevan, Niema M
Kheradvar, Arash

Publication Date
2015-10-01

DOI
10.1007/s10439-015-1302-y

Peer reviewed

Annals of Biomedical Engineering (© 2015)
DOI: 10.1007/s10439-015-1302-y

BMES BIOMEDICAL ENGINEERING SOCIETY™ www.bmes.org

Effect of the Mitral Valve's Anterior Leaflet on Axisymmetry of Transmitral Vortex Ring

AHMAD FALAHATPISHEH,[1,2] NIEMA M. PAHLEVAN,[3,4] and ARASH KHERADVAR[1,2]

[1]Department of Mechanical and Aerospace Engineering, University of California, Irvine, Irvine, USA; [2]Department of Biomedical Engineering, University of California, Irvine, Irvine, CA, USA; [3]Department of Medical Engineering, California Institute of Technology, Pasadena, CA, USA; and [4]Huntington Medical Research Institute, Pasadena, CA, USA

(*Received 8 January 2015; accepted 13 March 2015*)

Associate Editor Umberto Morbiducci oversaw the review of this article.

Abstract—The shape and formation of transmitral vortex ring are shown to be associated with diastolic function of the left ventricle (LV). Transmitral vortex ring is a flow feature that is observed to be non-axisymmetric in a healthy heart and its inherent asymmetry in the LV assists in efficient ejection of the blood during systole. This study is a first step towards understanding the effects of the mitral valve's anterior leaflet on transmitral flow. We experimentally study a single-leaflet model of the mitral valve to investigate the effect of the anterior leaflet on the axisymmetry of the generated vortex ring based on the three-dimensional data acquired using defocusing digital particle image velocimetry. Vortex rings form downstream of a D-shaped orifice in presence or absence of the anterior leaflet in various physiological stroke ratios. The results of the statistical analysis indicate that the formed vortex ring downstream of a D-shaped orifice is markedly non-axisymmetric, and presence of the anterior leaflet improves the ring's axisymmetry. This study suggests that the improvement of axisymmetry in presence of the anterior leaflet might be due to coupled dynamic interaction between rolling-up of the shear layer at the edges of the D-shaped orifice and the borders of the anterior leaflet. This interaction can reduce the non-uniformity in vorticity generation, which results in more axisymmetric behavior compared to the D-shaped orifice without the anterior leaflet.

Keywords—Mitral valve, Anterior leaflet, Non-axisymmetry, Vortex ring.

NOMENCLATURE

U_0	Plateau velocity of the piston
D	Equivalent diameter of the D-shaped orifice
L/D	Stroke ratio
ξ	Axisymmetry index
$\bar{I}$	Impulse threshold
$\bar{I}_<$	Average of the impulses less than the impulse threshold, $\bar{I}$
$\bar{I}_>$	Average of the impulses more than the impulse threshold, $\bar{I}$
N	Number of θ-planes
ω_θ	Vorticity distribution in each θ-plane
Re_Γ	Reynolds number of vortex ring
Γ_θ	Circulation in each θ-plane
Γ^*_θ	Non-dimensional circulation in each θ-plane
$\overline{\Gamma_\theta}^*$	Average of non-dimensional circulation in all θ-planes
R_θ	Radial vorticity centroid in each θ-plane
R^*_θ	Non-dimensional radial vorticity centroid in each θ-plane
$\overline{R_\theta}^*$	Average of non-dimensional radial vorticity centroid in all θ-planes
I_θ	Impulse in each θ-plane
I^*_θ	Non-dimensional impulse in each θ-plane
$\overline{I_\theta}^*$	Average of non-dimensional impulse in all θ-planes

INTRODUCTION

Recent advancements in cardiac imaging provide opportunities for 3D mapping of blood flow inside the

Address correspondence to Arash Kheradvar, Department of Biomedical Engineering, University of California, Irvine, Irvine, CA, USA. Electronic mail: arashkh@uci.edu

Published online: 28 March 2015

heart chambers. It has been previously shown that the flow pattern inside the heart and particularly in the left ventricle (LV) can represent a variety of cardiac dysfunctions.[41] One example is the vortex ring that develops along with the transmitral jet whose dynamics has been shown to be correlated with diastolic function.[19,38] Transmitral vortex ring is a flow feature that is observed to be asymmetric in a healthy heart.[19,26] The shape and dynamics of transmitral vortex ring are not only a measure of diastolic function[3,4,6,11,15,19,32] but also can be used as a tool to assess the mitral valve.[6,15,20] The inherent asymmetry of the vortex ring that is formed in a healthy LV helps ejection of the blood during systole.[1,19] Alternatively, unnatural asymmetry of the intraventricular flow may significantly reduce the LV's pumping efficiency.[34] However, no quantitative measure currently exists to assess the axisymmetry of transmitral vortex ring.

Recently, Falahatpisheh and Kheradvar introduced an index that measures the vortex rings' non-axisymmetry.[9] The index examines the impulse spectrum of the ring to determine the axisymmetry; vortex rings with a broad impulse spectrum tend to be less axisymmetric while the ones with a narrow spectrum are more axisymmetric. The index ranges between 0 and 1, which 1 refers to a perfect axisymmetric vortex ring.[9]

Compared to the symmetric geometry of the tri-leaflet valves, e.g. the aortic valve, nature has chosen the mitral valve to be the only asymmetric valve. Geometrical asymmetry in the natural mitral valve consists of a D-shaped orifice and the anterior leaflet, which has a wider surface compared to the posterior leaflet.[30,31,37,42]. As a first step towards understanding basic effect of the asymmetric shape of the mitral valve on the shape and axisymmetry of the transmitral vortex ring, we experimentally study a simplified model of the mitral valve. We characterize the formation of the three-dimensional vortex ring ejected downstream of a single-leaflet valve as a model of mitral valve's anterior leaflet. Ultimately, the role that the presence or absence of the valve's leaflet plays on the axisymmetry of the formed vortex ring is studied.

METHODS

Experimental Setup

A piston-cylinder arrangement immersed in a water tank of 870 × 430 × 360 mm^3 was used to generate vortex rings (Fig. 1). The piston displaced through the cylinder by a computer-controlled stepper-motor that generates a trapezoidal-shaped velocity profile. For our experiments, the piston was set to accelerate from zero to reach a plateau velocity of $U_0 = 40$ mm/s in 300 ms, and then remained steady to achieve the desired stroke ratios. The piston was programmed to rapidly decelerate to stop after the pulse in 300 ms. The generated vortex rings were far enough from the chamber's side walls to avoid any wall effects.

Single-Leaflet Valve

The piston expelled the fluid toward the opening of the cylinder where two different nozzles were investigated. Nozzle (A) is a model of the anterior D-shaped mitral valve annulus with a leaflet that was made according to the physiological dimensions and behavior of a natural mitral valve (Fig. 2a).[2] Outlet (B) was the same D-shaped annulus as (A) but without the anterior leaflet, as shown in Fig. 2b. The valve models were made of silicone rubber with 15 Shore A hardness, specific gravity of 1.18 g/cc, and tensile strength of 2.8 MPa. The thickness of the leaflet was chosen to be equal to that of a natural mitral valve (i.e., 0.5 mm). The diameter of the D-shaped orifice was equivalent to $D = \sqrt{4A_{\text{orifice}}/\pi} = 19.7$ mm. The opening of the model with anterior leaflet is shown in the Supplementary Video Clip. As the piston moved forward and pushed the fluid out of the orifice, the leaflet responded to the pulse from the piston and gradually deformed until a complete opening. The leaflet positioned horizontally parallel to the axis of the piston when it was fully open. The model with the leaflet was in fact one-piece silicone rubber that could open and close from its base. The dynamics of the leaflet opening was not considered and the velocity fields were captured with defocusing digital particle image velocimetry while the valve was fully open.

Experimental Conditions

The jet stroke ratio (L/D) was set to 2.5, 3.5, 4.0, 4.5, 5.0, and 6.0. L is the displacement that the piston traveled during acceleration, steady-state, and deceleration. The diameter of the model without the leaflet, D, is constant during the time of piston displacement. For the orifice with the leaflet, the valve's diameter changed as the valve opened. However, in calculation of the stroke ratio for the model with the anterior leaflet, we did not considered the time-varying geometry of the valve and used the orifice diameter at its complete opening, which is equal to that of the model without leaflet. These stroke ratios were selected according to the physiologic range of vortex formation times (VFTs), as shown to be clinically relevant in range of 3.3 to 5.5.[11,19,22]

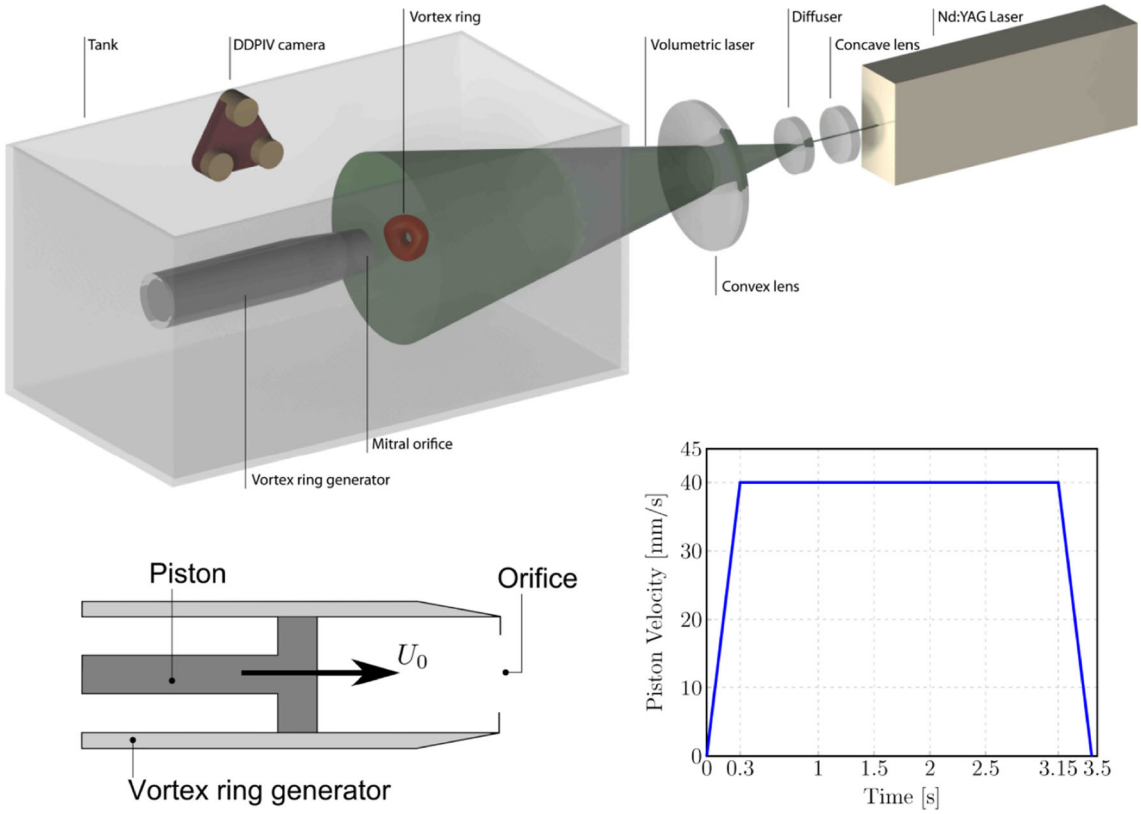

FIGURE 1. Schematic of the experimental set-up consists of an immersed piston-cylinder with the model of the mitral valve positioned at the outlet of the nozzle. The displacement of the piston is operated by a computer-controlled stepper motor that provides different stroke ratios. Downstream of the orifice is volumetrically illuminated by laser using optical lenses, which includes a diffuser, a concave and a convex lens. The DDPIV camera is placed outside of the tank perpendicular to the axis of the cylinder. A pulse/delay generator synchronizes both the camera and laser illumination for proper acquisitions. The piston velocity profile for $L/D = 6$ is also shown.

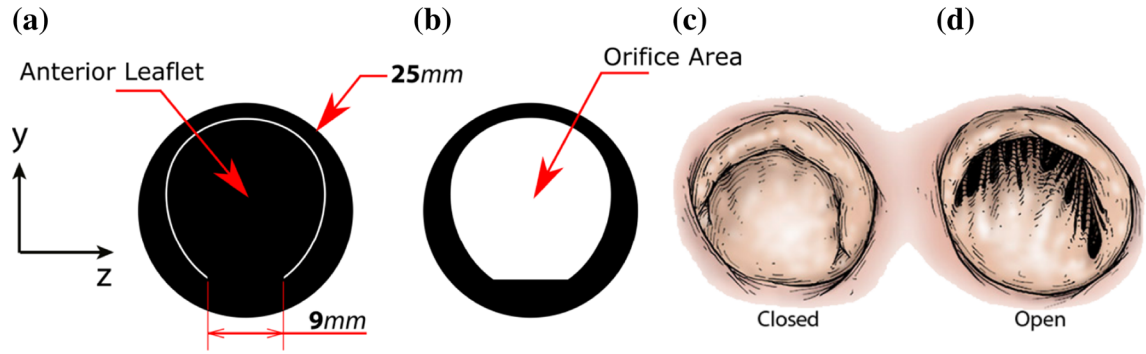

FIGURE 2. The geometry of the models; a single leaflet is approximated as the anterior leaflet since its motion is dominant compared to the posterior leaflet; (a) shows the mitral valve model with leaflet. The anterior leaflet is annotated. The orifice area forms as the anterior leaflet opens in a direction perpendicular to the plane (See the Supplementary Video); (b) represents the orifice when the leaflet is cut; (c) and (d) illustrate a normal mitral valve while it is open and closed, respectively (adapted from https://www.surgery.medsch.ucla.edu/cardiac/Clinical_Mitral%20Valve%20Replacement.shtml).

Defocusing Digital Particle Image Velocimetry (DDPIV)

The three-dimensional velocity fields were captured using DDPIV, as originally developed by Pereira and Gharib.[36] In DDPIV, particle depth information is determined by quantifying the natural blurring of the particle as it moves out of the focal plane and captured by three cameras. The defocusing PIV technique uses the image shift produced by the apertures to measure the depth of the particle from the camera. The DDPIV

system in this study utilizes a three-aperture mask arranged in the form of a triangle to eliminate the ambiguity in determining the depth. The DDPIV system is able to capture a volume of 100 × 100 × 100 mm^3 with 40,000 particles and 0.034 particles/pixel. Silver coated glass microspheres with the average diameter of 93 μm were used in this experiment.

The transmitral flow was captured up to 10 cm downstream of the valve apparatus, which is comparable to the transmitral jet passing through a native mitral valve toward LV's apex. The 3D velocity field for each stroke ratio was captured using the particle tracking velocimetry technique averaged over 30 identical cycles, where each cycle was duplicated with the same parameters. A total of 55 frames at the rate of 15 Hz were acquired for each experiment. The resolution of the velocity field was 39 × 39 × 39 in the domain of 100 × 100 × 100 mm^3. No smoothing was made in the resulted velocity and vorticity fields obtained by DDPIV. This set of experiments was conducted at the Gharib research lab at the California Institute of Technology.

Quantification of Vortex' Axisymmetry

We used the axisymmetry index, ξ, for vortex rings as described by Falahatpisheh and Kheradvar to quantify the shape of the 3D transmitral vortex rings.[9] This measure considers the vortex' impulse spectrum in several azimuthal planes (θ-planes), and is defined as[9]:

$$\xi = \frac{\bar{I}_<}{\bar{I}_>}, \tag{1}$$

where $\bar{I}_<$ is the average of the impulses smaller than the impulse threshold, $\bar{I}$, and $\bar{I}_>$ is the average of the impulses greater than the impulse threshold. Impulse threshold is calculated as[9]:

$$\bar{I} = \frac{1}{N}\sum_{i=1}^{N} \mathbf{I}_\theta, \tag{2}$$

where N is the number of θ-planes used to characterize the vortex ring; here, we used $N = 120$ θ-planes to assess the axisymmetry. $\mathbf{I}_\theta$ is the impulse in each θ-plane. We also calculated circulation, Γ_θ, radial vorticity centroid, R_θ, and impulse I_θ at each θ-planes according to[9]:

$$\Gamma_\theta = \int \omega_\theta \cdot dA_\theta \tag{3}$$

$$R_\theta = \frac{\int \sigma\omega_\theta dx d\sigma}{\int \omega_\theta dx d\sigma} \tag{4}$$

$$I_\theta = \pi\rho \int \omega_\theta \sigma^2 dx d\sigma, \tag{5}$$

where ω_θ is the vorticity distribution in the θ-plane, A_θ is the area of the θ-plane, and x and σ are the axial and radial coordinate, respectively. ρ is the density of the fluid, which was water in the present study. Impulses at different θ-planes were calculated with respect to the vorticity centroid at each timestep.[9]

Non-dimensionalization

Γ_θ and R_θ were non-dimensionalized as $\Gamma^*_\theta = \Gamma_\theta/(U_0 D)$, and $R^*_\theta = R_\theta/D$, respectively; consequently, $\overline{\Gamma_\theta}^* = \overline{\Gamma_\theta}/(U_0 D)$ and $\overline{R_\theta}^* = \overline{R_\theta}/D$. Impulse at each θ-plane was non-dimensionalized as $I^*_\theta = I_\theta/\left(\pi\rho\overline{\Gamma_\theta}\,\overline{R_\theta}^2\right)$; $\overline{I_\theta}^* = \overline{I_\theta}/\left(\pi\rho\overline{\Gamma_\theta}\,\overline{R_\theta}^2\right)$. Similar to the Reynolds number defined for axisymmetric rings,[12] we defined the Reynolds number of the formed non-axisymmetric rings using the averaged circulation in all θ-planes:

$$\mathrm{Re}_\Gamma = \overline{\Gamma_\theta}/\nu, \tag{6}$$

where ν is the kinematic viscosity of the fluid.

Statistical Analysis

A paired t-test was used to examine whether the presence of the leaflet has a statistically significant effect on axisymmetry of the vortex rings represented by ξ. We also examined the statistical significance of the difference in the mean non-dimensional circulation, $\overline{\Gamma_\theta}^*$, mean non-dimensional radial vorticity centroid, $\overline{R_\theta}^*$, mean non-dimensional impulse, $\overline{I_\theta}^*$, in presence or absence of the leaflet. Furthermore, a linear regression analysis was performed to quantify the effect of the leaflet, stroke ratio, and vortex evolution on the axisymmetry index, ξ, based on 36 experimental observations. A p-value less than 0.05 was considered statistically significant. Analyses were performed in MATLAB (MathWorks, Inc., Natick, MA).

RESULTS

Axisymmetry Index for Transmitral Vortices

Mitral Annulus with Anterior Leaflet

For each stroke ratio (L/D), we captured the vortex ring's evolution at three time-steps of formation, translation and steady state, which are based on the relative time evolution of the vortices. Formation refers to the time where the vortex ring formed in the vicinity of the orifice, translation refers to the time where the ring translated forward after it was formed, and lastly, steady state is when the ring evolved from translation to a steady state. We used $\omega = 2$ s^{-1} for all

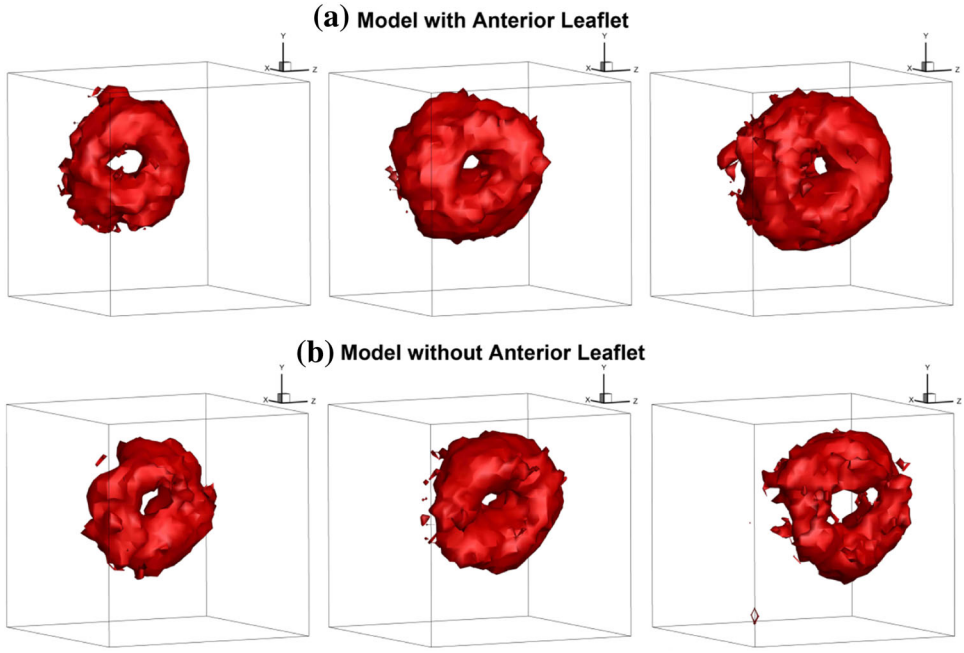

FIGURE 3. Vortex rings formed and translated downstream the model with (a) and without anterior leaflet (b) when $L/D = 3.5$ are also shown for iso-surfaces of $\omega = 2.0$. No smoothing was applied to the 3D velocity field.

the cases so that a complete ring could be visualized. The vortex rings illustrated by the iso-surfaces of the vorticity magnitude for $L/D = 3.5$ are shown in Fig. 3b as an example. The Reynolds number, Re_Γ, mean non-dimensional circulation, $\overline{\Gamma_\theta}^*$, mean non-dimensional radial vorticity centroid, $\overline{R_\theta}^*$, and mean non-dimensional impulse, $\overline{I_\theta}^*$, were computed for all the stroke ratios, as shown in Table 1. The circulation spectrum, radial vorticity centroid, and impulse are shown in Fig. 4 for $L/D = 6.0$, as an example.

Mitral Annulus with No Anterior Leaflet

For the D-shaped mitral annulus with no anterior leaflet, the effect of the leaflet was eliminated. Similar to the annulus with leaflet, we captured three vortex rings at different stages of formation, translation and steady state. The vortex rings for the stroke ratio of 3.5 are shown in Fig. 3c. The Reynolds number, Re_Γ, mean non-dimensional circulation, $\overline{\Gamma_\theta}^*$, mean non-dimensional radial vorticity centroid, $\overline{R_\theta}^*$, and mean non-dimensional impulse, $\overline{I_\theta}^*$, for all the stroke ratios are shown in Table 1. The spectrum of the circulation, radial vorticity centroid, and impulse for $L/D = 6.0$ during steady state stage is shown in Fig. 5.

The difference between the vortex ring's axisymmetry indices generated from the models with and without leaflet is shown in Fig. 6 and Table 2. The percent difference is calculated according to $= (\xi_{\text{with}} - \xi_{\text{without}})/\xi_{\text{without}} \times 100$. The red area is the region shaded between $\pm 5\%$ engineering error ranges. The results show that the majority of the absolute values of the difference were larger than 5%. In addition, the variation of axisymmetry index vs. stroke ratio is shown in Fig. 7 for both models with and without the leaflet.

Statistical Analysis Result

The p-values resulted from the paired t-test are shown in Table 3. The p-value for the mean non-dimensional circulation, $\overline{\Gamma_\theta}^*$, was found to be 0.0074, which is statistically significant. Consequently, there was no statistically significant difference in the rings' Reynolds numbers according to its definition, $\mathrm{Re}_\Gamma = \overline{\Gamma_\theta}^*/\nu$. The p-value for the mean non-dimensional radial vorticity centroid, $\overline{R_\theta}^*$, was found to be 0.2723, which is not statistically significant. The p-value for the mean non-dimensional impulse, $\overline{I_\theta}^*$, was found to be statistically significant ($p = 0.0042$). The p-value for the axisymmetry index was found to be 0.0013, which is statistically significant. The p-values resulted from the linear regression for the effect of the leaflet, stroke ratio, and evolution time were found to be 4.74×10^{-4}, 0.2917, and 4.93×10^{-9}, respectively, as shown in Table 4.

DISCUSSION

The intraventricular vortex ring that forms during the early transmitral flow propagates away from the

TABLE 1. Resulted values of Reynolds number of the vortex ring, $Re_\Gamma = \overline{\Gamma_\theta}/\nu$, non-dimensional circulation, $\Gamma^*_\theta = \Gamma_\theta/(U_0 D)$, non-dimensional radial vorticity centroid, $R^*_\theta = R_\theta/D$, non-dimensional impulse, $I^*_\theta = I_\theta/\left(\pi\rho\overline{\Gamma_\theta} R_\theta^2\right)$, and axisymmetry index, $\xi = \frac{I_<}{I_>}$, for two models: with the anterior leaflet and without the leaflet.

	$L/D = 2.5$ with leaflet			$L/D = 2.5$ without leaflet		
Re_Γ	2.33×10^3	3.09×10^3	3.63×10^3	1.85×10^3	3.02×10^3	4.08×10^3
Γ^*_θ	2.58 ± 0.14	3.42 ± 0.19	4.01 ± 0.15	2.04 ± 0.14	3.34 ± 0.18	4.51 ± 0.24
R^*_θ	0.86 ± 0.22	1.02 ± 0.21	1.15 ± 0.18	0.77 ± 0.40	0.99 ± 0.26	1.05 ± 0.23
I^*_θ	1.23 ± 0.59	1.23 ± 0.41	1.18 ± 0.28	1.46 ± 0.88	1.25 ± 0.64	1.20 ± 0.50
ξ	0.37	0.56	0.64	0.35	0.41	0.49
	$L/D = 3.5$ with leaflet			$L/D = 3.5$ with leaflet		
Re_Γ	2.10×10^3	3.52×10^3	4.76×10^3	1.87×10^3	3.19×10^3	3.84×10^3
Γ^*_θ	2.32 ± 0.16	3.90 ± 0.21	5.26 ± 0.22	2.07 ± 0.23	3.52 ± 0.20	4.25 ± 0.14
R^*_θ	0.74 ± 0.33	0.98 ± 0.23	1.03 ± 0.18	0.79 ± 0.30	1.03 ± 0.27	1.09 ± 0.19
I^*_θ	1.24 ± 1.12	1.21 ± 0.39	1.22 ± 0.31	1.33 ± 0.94	1.28 ± 0.56	1.25 ± 0.37
ξ	0.17	0.56	0.61	0.32	0.46	0.61
	$L/D = 4.0$ with leaflet			$L/D = 4.0$without leaflet		
Re_Γ	2.13×10^3	3.24×10^3	4.26×10^3	1.93×10^3	2.99×10^3	4.15×10^3
Γ^*_θ	2.36 ± 0.10	3.59 ± 0.23	4.71 ± 0.15	2.13 ± 0.36	3.31 ± 0.15	4.59 ± 0.19
R^*_θ	0.80 ± 0.25	1.00 ± 0.19	1.05 ± 0.19	0.83 ± 0.42	1.01 ± 0.26	1.05 ± 0.23
I^*_θ	1.14 ± 0.71	1.16 ± 0.32	1.19 ± 0.37	1.69 ± 1.13	1.24 ± 0.59	1.22 ± 0.50
ξ	0.33	0.61	0.54	0.31	0.46	0.51
	$L/D = 4.5$ with leaflet			$L/D = 4.5$ without leaflet		
Re_Γ	2.65×10^3	3.41×10^3	4.55×10^3	1.93×10^3	2.79×10^3	4.24×10^3
Γ^*_θ	2.93 ± 0.22	3.77 ± 0.17	5.03 ± 0.20	2.13 ± 0.26	3.08 ± 0.16	4.69 ± 0.14
R^*_θ	0.84 ± 0.20	1.01 ± 0.22	1.05 ± 0.20	0.77 ± 0.45	1.04 ± 0.36	1.06 ± 0.22
I^*_θ	1.16 ± 0.64	1.18 ± 0.40	1.19 ± 0.39	1.62 ± 1.41	1.21 ± 0.78	1.24 ± 0.41
ξ	0.39	0.54	0.51	0.20	0.33	0.58
	$L/D = 5.0$ with leaflet			$L/D = 5.0$ without leaflet		
Re_Γ	2.53×10^3	3.36×10^3	4.52×10^3	2.26×10^3	3.28×10^3	3.91×10^3
Γ^*_θ	2.80 ± 0.16	3.72 ± 0.17	5.00 ± 0.15	2.49 ± 0.23	3.63 ± 0.25	4.32 ± 0.23
R^*_θ	0.89 ± 0.18	1.00 ± 0.24	1.05 ± 0.17	0.82 ± 0.39	0.98 ± 0.30	1.05 ± 0.27
I^*_θ	1.23 ± 0.59	1.17 ± 0.44	1.19 ± 0.31	1.36 ± 1.05	1.30 ± 0.64	1.23 ± 0.52
ξ	0.44	0.46	0.64	0.25	0.42	0.48
	$L/D = 6.0$ with leaflet			$L/D = 6.0$ without leaflet		
Re_Γ	2.70×10^3	3.80×10^3	4.72×10^3	3.07×10^3	3.31×10^3	4.92×10^3
Γ^*_θ	2.98 ± 0.16	4.20 ± 0.15	5.22 ± 0.20	3.40 ± 0.28	3.66 ± 0.17	5.44 ± 0.16
R^*_θ	0.89 ± 0.15	0.98 ± 0.15	1.09 ± 0.15	0.84 ± 0.22	0.99 ± 0.26	1.04 ± 0.21
I^*_θ	1.17 ± 0.42	1.24 ± 0.38	1.19 ± 0.22	1.28 ± 0.80	1.24 ± 0.63	1.23 ± 0.39
ξ	0.56	0.60	0.73	0.32	0.40	0.58

The reported values for Γ^*_θ, R^*_θ, and I^*_θ are the mean and standard deviation. Three columns in each group represent three stages of ring's evolution.

mitral valve's leaflets. It entrains the intraventricular ambient fluid until it is pinched-off from the transmitral jet.[19] Mainly through contrast echocardiography, echo-PIV[23] and 4D Flow MR,[29] it has been observed that the forming transmitral vortex ring possesses a non-axisymmetric shape as illustrated in Fig. 8.[18,19,35,40] The sources of transmitral vortex' asymmetry include D-shaped orifice, larger anterior leaflet, and mitral valve's location, which is slightly closer to the LV lateral wall compared to the interventricular wall. However, no study has quantitatively investigated the effects of these sources on vortex' asymmetry.

Here we quantitatively measured the axisymmetry of vortex ring formed downstream of a model of a mitral valve when the effect of the wall is removed in a piston-cylinder mechanism. If we consider the

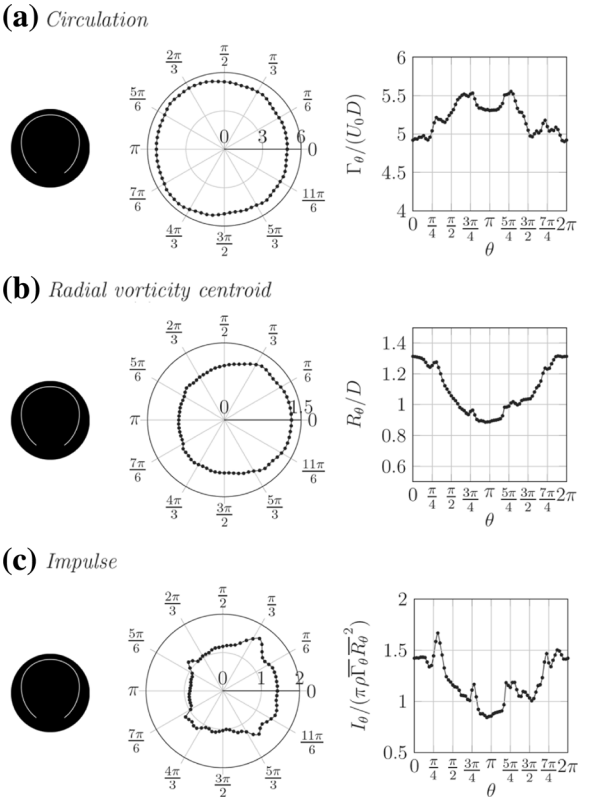

FIGURE 4. Spectrum of the circulation, Γ_θ, radial vorticity centroid, R_θ, and impulse, I_θ, non-dimensionalized for the non-axisymmetric vortex ring created downstream of the model with leaflet at $L/D = 6.0$ in the steady state stage. The model with anterior leaflet is also shown as a reference. The left figures represent a polar distribution while the ones on the right are a linear distribution vs. the angle each θ-plane makes with respect to the *xy*-plane. The axisymmetry index for this vortex ring is $\xi = 0.73$.

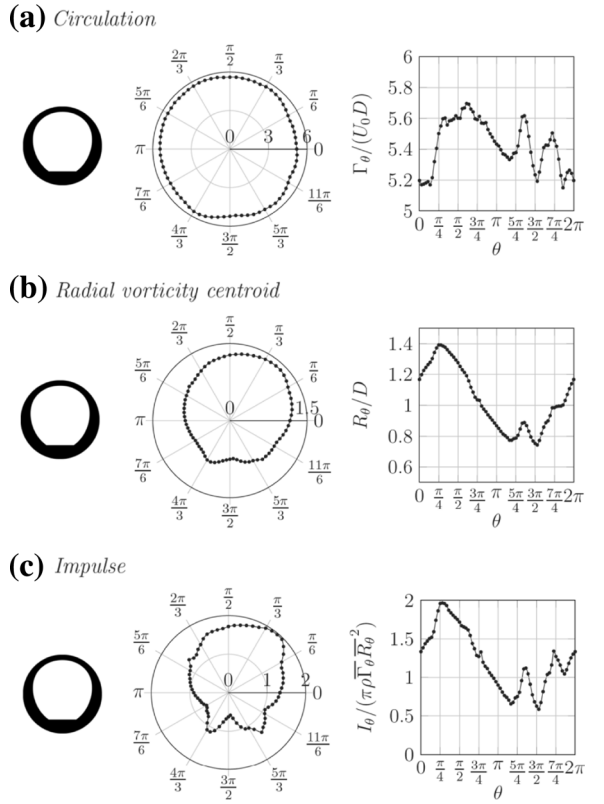

FIGURE 5. Spectrum of the circulation, Γ_θ, radial vorticity centroid, R_θ, and impulse, I_θ, non-dimensionalized for the non-axisymmetric vortex ring created downstream of the model without leaflet at $L/D = 6.0$ in the steady state stage. The model without the anterior leaflet is also shown as a reference. The left figures represent a polar distribution while the ones on the right are a linear distribution vs. the angle each θ-plane makes with respect to the *xy*-plane. The axisymmetry index for this vortex ring is $\xi = 0.58$.

grouping of the left atrium (LA) and LV equivalent to a piston-cylinder mechanism, transmitral flow is a forward moving flow from LA to LV, regardless of whether the piston being pulled toward LV (early diastole) or pushes toward the LV (atrial contraction). What makes a difference to the developed vortex ring is the timing of the ejection, previously described as vortex formation time.[12,21,24] Additionally, the shape of the ring from an axisymmetric perspective is not affected by pulling or pushing the piston but rather is affected by the shape and dynamics of the orifice. Accordingly, the effect of the anterior leaflet on vortex axisymmetry was studied using the axisymmetry index.[9] In presence or absence of the anterior leaflet, the deviations of the vortex rings from axisymmetry were compared for a variety of stroke ratios and at three different stages of vortex evolution: formation, translation and steady state.

Effect of the D-Shaped Annulus

The geometrical difference between a circular orifice and D-shaped annulus is that the former possesses a uniform curvature while the latter has a variable curvature along its edges. This affects rolling-up of the shear layer and process of vortex formation.[5] The changes of the local curvature at the edges of the D-shaped orifice compared to a circular orifice are the source of disturbance for the ring formation. Therefore, non-uniform rolling up of the shear layer makes the formed vortex ring less axisymmetric when compared to the one ejected from a circular nozzle. Shape of the D-shape of the nozzle may vary from valve to valve. In the present study, the mitral valve's non-circular orifice (D-shaped) was considered with a physiologic orifice area. Curvature of the D-shaped orifice may affect the axisymmetry of the vortex ring, which we did not test in this study.

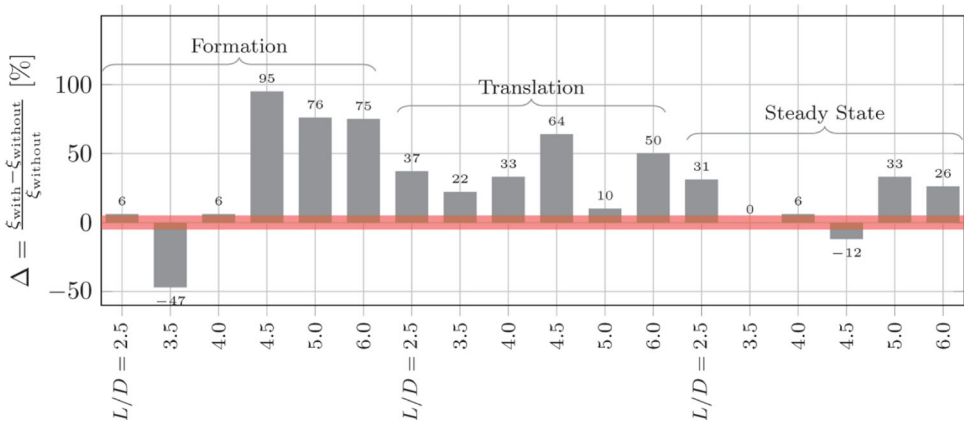

FIGURE 6. Difference between the axisymmetry index of the vortex ring generated by the models with and without the leaflet. The percent difference is calculated according to $= (\xi_{with} - \xi_{without})/\xi_{without} \times 100$. The red area is the region shaded between ±5% error. The majority of the absolute value of the differences were larger than 5%.

TABLE 2. Difference between the axisymmetry index of the vortex ring generated by the models with and without the leaflet.

	ξ_{with}	$\xi_{without}$	Δ (%)
Step I of evolution			
$L/D = 2.5$	0.37	0.35	6
$L/D = 3.5$	0.17	0.32	−47
$L/D = 4.0$	0.33	0.31	6
$L/D = 4.5$	0.39	0.20	95
$L/D = 5.0$	0.44	0.25	76
$L/D = 6.0$	0.56	0.32	75
Step 2 of evolution			
$L/D = 2.5$	0.56	0.41	37
$L/D = 3.5$	0.56	0.46	22
$L/D = 4.0$	0.61	0.46	33
$L/D = 4.5$	0.54	0.33	64
$L/D = 5.0$	0.46	0.42	10
$L/D = 6.0$	0.60	0.40	50
Step 3 of evolution			
$L/D = 2.5$	0.64	0.49	31
$L/D = 3.5$	0.61	0.61	0
$L/D = 4.0$	0.54	0.51	6
$L/D = 4.5$	0.51	0.58	−12
$L/D = 5.0$	0.64	0.48	33
$L/D = 6.0$	0.73	0.58	26

The percent difference is calculated according to $= (\xi_{with} - \xi_{without})/\xi_{without} \times 100$.

Mitral Valve as a Three Dimensional Complex Orifice

The shape of the mitral valve is atypical compared to the other three heart valves. Anatomic geometry of the mitral valve makes it a complex three-dimensional orifice[39] whose asymmetric shape of the anterior leaflet and the non-axisymmetric D-shaped geometry of its annulus contribute to non-uniform vorticity generation. The vortex ring forming downstream of the mitral valve is linked to this highly time-dependent non-uniform vorticity generation during the opening of the valve.

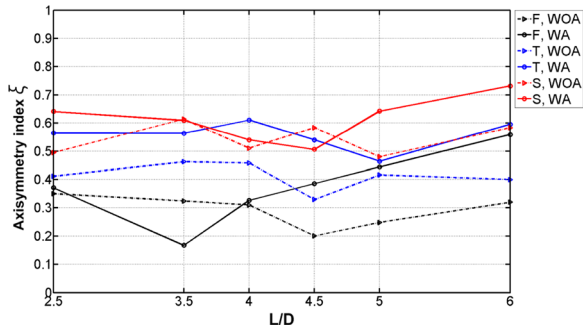

FIGURE 7. Axisymmetry vs. stroke ratio for both models with and without leaflet at different stages of the evolution. *F*, *T*, and *S* represent formation, translation, and steady state and WA and WOA refer to models with and without anterior leaflet, respectively.

TABLE 3. Results of *t*-test for mean non-dimensional circulation, $\overline{\Gamma_\theta}^*$, mean non-dimensional radial vorticity centroid, $\overline{R_\theta}^*$, mean non-dimensional impulse, $\overline{I_\theta}^*$, and axisymmetry index, ξ.

	h	*p*-value	CI	t_{stat}	*df*	SD
$\overline{\Gamma_\theta}^*$	1	0.0074	[0.0880, 0.4865]	3.0409	17	0.4008
$\overline{R_\theta}^*$	0	0.2723	[−0.0112, 0.0373]	1.1346	17	0.0487
$\overline{I_\theta}^*$	1	0.0042	[−0.1933, −0.0426]	−3.3025	17	0.1515
ξ	1	0.0013	[0.0441, 0.1520]	3.8333	17	0.1085

h is result of the hypothesis, *p* is the *p*-value, CI is the confidence interval, t_{stat} is the value of the test statistic, *df* is the degrees of freedom, and SD is the standard deviation.

TABLE 4. Results of linear regression.

	Coefficients	Standard error	*t* Stat	*p*-value
(Intercept)	0.0225	0.0698	0.3219	0.7496
Leaflet	0.0981	0.0252	3.8921	0.0005
Stroke ratio	0.0122	0.0114	1.0723	0.2916
Stage of evolution	0.1221	0.0154	7.9157	4.93×10^{-9}

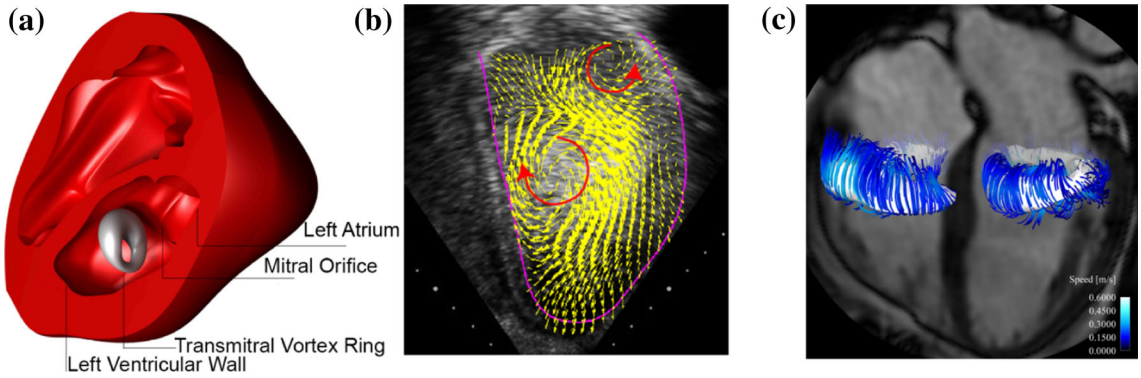

FIGURE 8. Transmitral vortex ring. (a) a 3D schematic of a naturally-formed transmitral vortex ring, which is non-axisymmetric; (b) a 2D echocardiographic-PIV image of a normal left ventricle in mid-diastole shows a transmitral vortex formed asymmetrically shown by two red arrows; (c) illustrates the non-axisymmetric vortex ring formed in the left and right ventricles obtained by 4D-Flow MRI; the image is courtesy of Dr. Tino Ebbers, and is adapted from Kheradvar and Pedrizzetti (see Chap. 5, Fig. 5.4.b).[25]

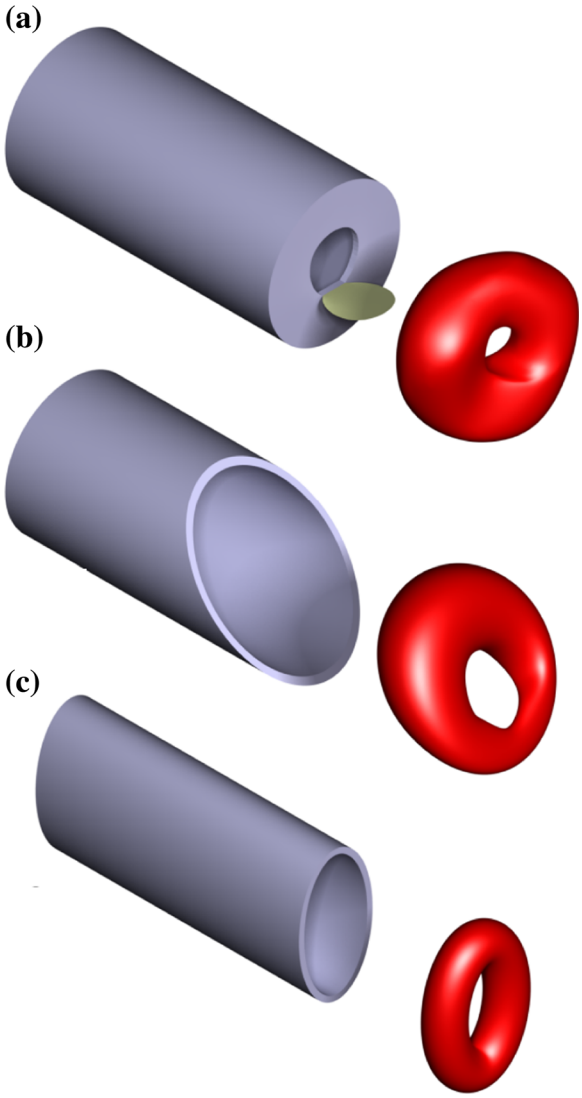

FIGURE 9. Comparison of the mitral valve orifice nozzle with other non-axisymmetric vortex ring generators. (a) The single-leaflet valve model used in this study; (b) an inclined nozzle with a circular cross section;[27] (c) a vortex ring generator with an elliptical cross section.

Compared to the previously-studied nozzles that generate non-axisymmetric vortex ring in a piston-cylinder mechanism,[7,13,14,16,27,43] the valve model used in this study has a distinct 3D feature. These vortex generator setups are as shown in Fig. 9. Le *et al.*[27] numerically studied the dynamics of a laminar vortex in impulsively driven flows through inclined nozzles in a piston–cylinder apparatus. The schematic of the formed vortex ring is shown in Fig. 9b. Also, the schematic of the vortex ring formed downstream of an elliptical nozzle is shown in Fig. 9c. Compared to the nozzles in Figs. 9b and 9c and during the valve opening, the regions from which vorticity is generated in the single-leaflet valve do not lie in a single plane while having a non-stationary exit during fluid ejection. In other words, as the valve progressively opens, these regions from which vorticity generates dynamically relocate to a new position that consequently alters the shape of the formed vortex ring. In our simplified model of the mitral valve, we did not account for the mitral valve's dynamic, the posterior leaflet, and the interaction of the formed vortex ring with the left ventricular wall. These effects were beyond the scope of this work.

Effect of the Anterior Leaflet on the Transmitral Vortex Ring

Based on the paired *t*-test, the anterior leaflet significantly affected the axisymmetry of the vortex when compared to the D-shaped annulus without the anterior leaflet (p-value = 0.0013). In fact, the axisymmetry of the vortex ring was shown to be improved by the presence of the leaflet, as illustrated in Table 4. This can be also observed by examining the spectrum of the circulation, radial vorticity centroid and the rings' impulse, which highlight the difference between the rings formed downstream of the two orifices, as shown in Figs. 4 and 5. Broader spectrums for the D-shaped

orifice without leaflet are associated with a larger deviation of the ring from axisymmetry. Furthermore, as the vortex ring evolved downstream of the orifice, the average magnitude of difference in axisymmetry between the two rings monotonically decreased along with an increase in the circulation (Table 4). This difference decreased from 50.8% at the formation stage to 36% during the translation stage that even further reduced to 18% at the steady state stage.

The formed vortex ring was observed to be severely non-axisymmetric at the formation stage, for both models with and without leaflet, as shown in Table 1. In presence of the anterior leaflet and for all the studied stroke ratios, the ring at the formation stage possessed a range of 17–56% axisymmetry and the annulus without leaflet had a range of 20–35% axisymmetry. This shows that at the formation stage both models generate significantly non-axisymmetric vortex rings. However, compared to the formation stage, this non-axisymmetry decreased during the ring's evolution and forward translation along with an increased circulation at the steady state stage, as can be deducted from Table 1. Since the ring's circulation monotonically increases during the evolution and forward translation, we hypothesize that the vortex's axisymmetry would be optimal at the onset of pinch-off where the circulation is saturated.[12] It was also observed that the effect of the stroke ratio on axisymmetry was statistically insignificant. This implies that vortex formation time in the studied range, which covers normal and diseased LVs, is irrelevant to the shape of the ring.

Based on our experimental results, we hypothesize that the improvement of axisymmetry in presence of the anterior leaflet is due to coupled dynamic interaction of rolling-up of the shear layer at the edges of the D-shaped orifice with the borders of the anterior leaflet. This interaction seems to reduce the non-uniformity in the vorticity generation , which results in more axisymmetric behavior compared to the D-shaped orifice with no anterior leaflet.

Potential Clinical Application

Several previous studies have emphasized that the transmitral jet's stroke ratio or vortex formation time significantly and reliably changes in a variety of cardiac dysfunctions[11,17,19,28] and valve diseases.[22,33] However, due to lack of imaging capabilities for mapping the transmitral vortex ring in 3D, the shape effect and axisymmetry of the ring have not yet studied *in vivo*. With recent advancement in 3D Echo-PIV[8,10] and 4D Flow MRI,[29] it is anticipated that shape of the transmitral vortex ring being further studied and compared in different cardiac conditions in near future. The vortex axisymmetry index is a non-dimensional number that can be compared among the patients and normal population once 3D LV flow field is obtained. Healthy ventricle possesses a non-axisymmetric mitral vortex.[23,31] However, it is not yet known which range or value of axisymmetry is normal or optimal. We anticipate that the axisymmetry of the formed vortex ring in normal subjects lies within a physiological range that should be studied in normal population and compared to the values to be measured in different cardiac conditions.

LIMITATIONS

Measurement errors may exist due to the noise in the DDPIV data and motor vibration, which may have slightly affected the calculation of ring's centroid. Due to frame-rate limitation of the DDPIV, only three time-steps of the vortex ring were captured, and as a result, some of the transitional stages may have not been imaged. The orifice of the native mitral valve is elliptical, three-dimensional, and saddle-shaped rather than flat as used in the present study. Additionally, this study was only focused on the effects of the anterior leaflet on transmitral vortex' shape and did not consider the interaction of the vortex with LV walls, which has been previously shown to affect vortex axisymmetry.[20] Posterior leaflet was not modeled in our study since from an experimental perspective, creating models with and without the posterior leaflet is not practical mainly because the model without the posterior leaflet will lose its integrity. Using water along with other physiologically based values might cause deviation from physiological Reynolds number. This deviation in Reynolds number may affect circulation and vorticity generated in the vortex ring, and therefore, might result in a different axisymmetry index. However, the present study was aimed to compare vortex' axisymmetry ejected in presence and absence of the anterior leaflet while keeping everything else the same, and therefore we expect that the relative differences would be the same.

CONCLUSIONS

In this study, we examined the effect of the anterior leaflet in a simplified model of mitral valve. A single-leaflet valve model was used in a vortex generator setup along with using defocusing digital particle image velocimetry to obtain three-dimensional velocity fields. We studied the shape of the formed vortex ring downstream of the valve at different stages of formation. We quantitatively measured the vortex' axisymmetry ejected from a D-shaped annulus with and

without the anterior leaflet (Fig. 2). The vortex rings ejected from a D-shaped annulus were found to be non-axisymmetric. This study suggests that, in the absence of the mitral valve's posterior leaflet, annulus dynamics, and the left ventricular wall interaction, the main source of vortex' non-axisymmetry is the D-shaped annulus, and presence of the anterior leaflet improves the vortex' axisymmetry. We hypothesize that the dynamic interaction of the shear layer rolling-up from the edges of the anterior leaflet with the one on the D-shaped edge of the orifice reduces the non-uniformity in vorticity generation. This reduction is with respect to the non-uniform vorticity that was generated downstream of the model with no anterior leaflet. A potential clinical application of the axisymmetry index is to diagnose subtle diastolic dysfunction based on the shape and formation of transmitral vortex ring.

ELECTRONIC SUPPLEMENTARY MATERIAL

The online version of this article (doi:10.1007/s10439-015-1302-y) contains supplementary material, which is available to authorized users.

ACKNOWLEDGMENTS

This work was supported by the American Heart Association awards 14POST20530013 and 14GRNT 18800013 to Dr. Ahmad Falahatpisheh and Prof. Arash Kheradvar, respectively. The authors are also grateful to Prof. Morteza Gharib who generously allowed using his DDPIV setup at Caltech.

REFERENCES

[1]Abe, H., G. Caracciolo, A. Kheradvar, G. Pedrizzetti, B. K. Khandheria, and J. Narula. Sengupta PP. Contrast echocardiography for assessing left ventricular vortex strength in heart failure: a prospective cohort study. *Eur. Heart J. Cardiovasc. Imaging* 14(11):1049–1060, 2013.

[2]Carpentier, A., D. H. Adams, and F. Filsoufi. Carpentier's Reconstructive Valve Surgery. Philadelphia: Elsevier Health Sciences, 2011.

[3]Charonko, J., R. Kumar, K. Stewart, W. Little, and P. Vlachos. Vortices formed on the mitral valve tips aid normal left ventricular filling. *Ann. Biomed. Eng.* 41:1049–1061, 2013.

[4]de Vecchi, A., D. A. Nordsletten, E. W. Remme, H. Bellsham-Revell, G. Greil, J. M. Simpson, R. Razavi, and N. P. Smith. Inflow typology and ventricular geometry determine efficiency of filling in the hypoplastic left heart. *Ann. Thorac. Surg.* 94:1562–1569, 2012.

[5]Domenichini, F. Three-dimensional impulsive vortex formation from slender orifices. *J. Fluid Mech.* 666:506–520, 2011.

[6]Du, D., S. Jiang, Z. Wang, Y. Hu, and Z. He. Effects of suture position on left ventricular fluid mechanics under mitral valve edge-to-edge repair. *Biomed. Mater. Eng.* 24:155–161, 2014.

[7]Falahatpisheh, A., and A. Kheradvar. On axisymmetry of vortex rings. *Bull. Am. Phys Soc.* 59:418, 2014.

[8]Falahatpisheh, A., and A. Kheradvar. Volumetric echocardiographic particle image velocimetry (v-echo-piv). *Circulation*. 130:A14952, 2014.

[9]Falahatpisheh, A., and A. Kheradvar. A measure of axisymmetry for vortex rings. *Eur. J. Mech. B.* 49(Part A):264–271, 2015.

[10]Falahatpisheh, A., G. Pedrizzetti, and A. Kheradvar. Three-dimensional reconstruction of cardiac flows based on multi-planar velocity fields. *Experiments in Fluids*. 55:1848, 2014.

[11]Gharib, M., E. Rambod, A. Kheradvar, D. J. Sahn, and J. O. Dabiri. Optimal vortex formation as an index of cardiac health. *Proc. Natl. Acad. Sci. USA* 103:6305–6308, 2006.

[12]Gharib, M., E. Rambod, and K. Shariff. A universal time scale for vortex ring formation. *J. Fluid Mech.* 360:121–140, 1998.

[13]Grinstein, F. F. Vortex dynamics and entrainment in rectangular free jets. *J. Fluid Mech.* 437:69–101, 2001.

[14]Ho, C.-M., and E. Gutmark. Vortex induction and mass entrainment in a small-aspect-ratio elliptic jet. *J. Fluid Mech.* 179:383–405, 1987.

[15]Hu, Y., L. Shi, S. Parameswaran, S. Smirnov, and Z. He. Left ventricular vortex under mitral valve edge-to-edge repair. *Cardiovasc. Eng. Technol.* 1:235–243, 2010.

[16]Husain, H. S., and F. Hussain. Elliptic jets. Part 2. Dynamics of coherent structures: pairing. *J. Fluid Mech.* 233:439–482, 1991.

[17]Jiamsripong, P., M. Alharthi, A. Calleja, E. McMahon, M. Katayama, J. Westerdale, M. Milano, J. Heys, F. Mookadam, and M. Belohlavek. Impact of pericardial adhesions on diastolic function as assessed by vortex formation time, a parameter of transmitral flow efficiency. *Cardiovasc. Ultrasound* 8:42, 2010.

[18]Jiamsripong, P., A. M. Calleja, M. S. Alharthi, M. Dzsinich, E. M. McMahon, J. J. Heys, M. Milano, P. P. Sengupta, B. K. Khandheria, and M. Belohlavek. Impact of acute moderate elevation in left ventricular afterload on diastolic transmitral flow efficiency: analysis by vortex formation time. *J. Am. Soc. Echocardiogr.* 22:427–431, 2009.

[19]Kheradvar, A., R. Assadi, A. Falahatpisheh, and P. P. Sengupta. Assessment of transmitral vortex formation in patients with diastolic dysfunction. *J. Am. Soc. Echocardiogr.* 25:220–227, 2012.

[20]Kheradvar, A., and A. Falahatpisheh. The effects of dynamic saddle annulus and leaflet length on transmitral flow pattern and leaflet stress of a bileaflet bioprosthetic mitral valve. *J. Heart Valve Dis.* 21:225, 2012.

[21]Kheradvar, A., and M. Gharib. Influence of ventricular pressure drop on mitral annulus dynamics through the process of vortex ring formation. *Ann. Biomed. Eng.* 35:2050–2064, 2007.

[22]Kheradvar, A., and M. Gharib. On mitral valve dynamics and its connection to early diastolic flow. *Ann. Biomed. Eng.* 37:1–13, 2009.

[23]Kheradvar, A., H. Houle, G. Pedrizzetti, G. Tonti, T. Belcik, M. Ashraf, J. R. Lindner, M. Gharib, and D. Sahn.

Echocardiographic particle image velocimetry: a novel technique for quantification of left ventricular blood vorticity pattern. *J. Am. Soc. Echocardiogr.* 23:3102–3111, 2010.
[24]Kheradvar, A., M. Milano, and M. Gharib. Correlation between vortex ring formation and mitral annulus dynamics during ventricular rapid filling. *ASAIO J.* 53:8–16, 2007.
[25]Kheradvar, A., and G. Pedrizzetti. Vortex Formation in the Cardiovascular System. New York: Springer, 2012.
[26]Kilner, P. J., G.-Z. Yang, A. J. Wilkes, R. H. Mohiaddin, D. N. Firmin, and M. H. Yacoub. Asymmetric redirection of flow through the heart. *Nature* 404:759–761, 2000.
[27]Le, T. B., I. Borazjani, S. Kang, and F. Sotiropoulos. On the structure of vortex rings from inclined nozzles. *J. fluid Mech.* 686:451–483, 2011.
[28]Mangual, J. O., E. Kraigher-Krainer, A. De Luca, L. Toncelli, A. Shah, S. Solomon, G. Galanti, F. Domenichini, and G. Pedrizzetti. Comparative numerical study on left ventricular fluid dynamics after dilated cardiomyopathy. *J. Biomech.* 46:1611–1617, 2013.
[29]Markl, M., P. Kilner, and T. Ebbers. Comprehensive 4d velocity mapping of the heart and great vessels by cardiovascular magnetic resonance. *J. Cardiovasc. Magn. Reson.* 13:7, 2011.
[30]McCarthy, K. P., L. Ring, and B. S. Rana. Anatomy of the mitral valve: understanding the mitral valve complex in mitral regurgitation. *Eur. J. Echocardiogr.* 11(10):i3–i9, 2010.
[31]Misfeld, M., and H.-H. Sievers. Heart valve macro- and microstructure. *Philos. Trans. R. Soc. B* 362:1421–1436, 2007.
[32]Nucifora, G., V. Delgado, M. Bertini, N. A. Marsan, N. R. Van de Veire, A. C. T. Ng, H.-M. J. Siebelink, M. J. Schalij, E. R. Holman, P. P. Sengupta, and J. J. Bax. Left ventricular muscle and fluid mechanics in acute myocardial infarction. *Am. J. Cardiol.* 106:1404–1409, 2010.
[33]Pagel, P. S., and J. A. Hudetz. Chronic pressure-overload hypertrophy attenuates vortex formation time in patients with severe aortic stenosis and preserved left ventricular systolic function undergoing aortic valve replacement. *J. Cardiothorac. Vasc. Anesth.* 27:660–664, 2013.
[34]Pedrizzetti, G., and F. Domenichini. Nature optimizes the swirling flow in the human left ventricle. *Phys. Rev. Lett.* 95:108101, 2005.
[35]Pedrizzetti, G., G. La Canna, O. Alfieri, and G. Tonti. The vortex—an early predictor of cardiovascular outcome? *Nat. Rev. Cardiol.* 11:545–553, 2014.
[36]Pereira, F., and M. Gharib. Defocusing digital particle image velocimetry and the three-dimensional characterization of two-phase flows. *Meas. Sci. Technol.* 13:683–694, 2002.
[37]Perloff, J. K., and W. C. Roberts. The mitral apparatus functional anatomy of mitral regurgitation. *Circulation.* 46:227–239, 1972.
[38]Poh, K. K., L. C. Lee, L. Shen, E. Chong, Y. L. Tan, P. Chai, T. C. Yeo, and M. J. Wood. Left ventricular fluid dynamics in heart failure: echocardiographic measurement and utilities of vortex formation time. *Eur. J. Echocardiogr.* 13:385–393, 2011.
[39]Salgo, I. S., J. H. Gorman, R. C. Gorman, B. M. Jackson, F. W. Bowen, T. Plappert, M. G. St John Sutton, and L. H. Edmunds. Effect of annular shape on leaflet curvature in reducing mitral leaflet stress. *Circulation.* 106:711–717, 2002.
[40]Schenkel, T., M. Malve, M. Reik, M. Markl, B. Jung, and H. Oertel. Mri-based cfd analysis of flow in a human left ventricle: methodology and application to a healthy heart. *Ann. Biomed. Eng.* 37:503–515, 2009.
[41]Sengupta, P. P., G. Pedrizzetti, P. J. Kilner, A. Kheradvar, T. Ebbers, G. Tonti, A. G. Fraser, and J. Narula. Emerging trends in CV flow visualization. *JACC Cardiovasc. Imaging* 5:305–316, 2012.
[42]Van Mieghem, N. M., N. Piazza, R. H. Anderson, A. Tzikas, K. Nieman, L. E. De Laat, J. S. McGhie, M. L. Geleijnse, T. Feldman, P. W. Serruys, and P. P. de Jaegere. Anatomy of the mitral valvular complex and its implications for transcatheter interventions for mitral regurgitation. *J. Am. Coll. Cardiol.* 56:617–626, 2010.
[43]Wlezien, R., and V. Kibens. Passive control of jets with indeterminate origins. *AIAA J.* 24:1263–1270, 1986.